PCCP

PAPER

View Article Online
View Journal | View Issue

Cite this: *Phys. Chem. Chem. Phys.*, 2014, **16**, 10990

Pressure dependent OH yields in the reactions of CH_3CO and $HOCH_2CO$ with O_2

C. B. M. Groß, T. J. Dillon† and J. N. Crowley*

Received 14th March 2014,
Accepted 15th April 2014

DOI: 10.1039/c4cp01108b

www.rsc.org/pccp

OH-formation in the reactions of CH_3CO (R1) and $HOCH_2CO$ (R4) with O_2 was studied in He, N_2 and air (27 to 400 mbar) using OH-detection by laser induced fluorescence (LIF). 248 nm laser photolysis of $COCl_2$ in the presence of CH_3CHO or $HOCH_2CHO$ was used as source of the acyl radicals CH_3CO and $HOCH_2CO$. The LIF-system was calibrated in back-to-back experiments by the 248 nm laser photolysis of H_2O_2 as OH radical precursor. A straight-forward analytical expression was used to derive OH yields (α) for both reactions. A Stern–Volmer-analysis results in $\alpha_{1b}^{-1}(N_2) = 1 + (9.4 \pm 1.7) \times 10^{-18}$ cm^3 molecule^{-1} $\times$ [M], $\alpha_{1b}^{-1}(He) = 1 + (3.6 \pm 0.6) \times 10^{-18}$ cm^3 molecule^{-1} $\times$ [M] and $\alpha_{4b}^{-1}(N_2) = 1 + (1.85 \pm 0.38) \times 10^{-18}$ cm^3 molecule^{-1} $\times$ [M]. Our results for CH_3CO are compared to the previous (divergent) literature values whilst that for $HOCH_2CO$, for which no previous data were available, provide some insight into the factors controlling the yield of OH in these reactions.

1 Introduction

Acetyl radicals (CH_3CO) play an important role in atmospheric chemistry. Important sources of acetyl radicals are the photolysis of acetone in the upper troposphere and the reaction of acetaldehyde with OH in the troposphere. The hydroxyl-substituted hydroxy acetyl radicals ($HOCH_2CO$) are formed in the reaction of OH with glycol aldehyde ($HOCH_2CHO$). The only significant reaction of acetyl and hydroxy acetyl radicals in the atmosphere is with O_2, forming (mainly) peroxy radicals. Accompanying peroxy radical formation, (R1) displays a second reaction pathway forming OH and an organic by-product. The branching ratio (α) for formation of OH increases from small values (<2%) at standard pressure to unity at pressures close to zero.[1,2]

$$CH_3CO + O_2 + M \rightarrow CH_3C(O)O_2 + M \quad (R1a)$$

$$\rightarrow OH + c\text{-}CH_2C(O)O \quad (R1b)$$

Reaction (R1) is considered to proceed *via* an excited peroxy radical $CH_3C(O)O_2^{\#}$ that is either stabilised by collisions with the bath gas molecules M or decomposes to form OH.[2–9] This is illustrated in reaction Scheme 1 (R = CH_3). The pressure dependence of α thus originates from the competition between the pressure- and bath gas-dependent quenching rate [M] $\times$ k_M and the pressure-independent decomposition rate k_D. A kinetic (Stern–Volmer) analysis of the reaction scheme leads to eqn (1) which can be used to parameterise α:

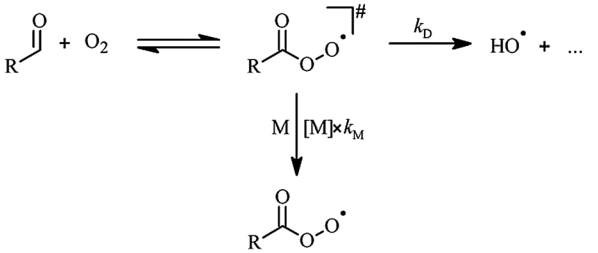

Scheme 1 Generalised mechanism for the reactions of CH_3CO (R = CH_3) and $HOCH_2CO$ (R = $HOCH_2$) with O_2.

$$\alpha^{-1} = 1 + \frac{k_M}{k_D}[M] \quad (1)$$

Although OH yields are low at pressures typical for the troposphere, (R1b) has an indirect impact on atmospheric chemistry because of its occurrence in laboratory experiments. The OH product of (R1b) has, for example, been used as spectroscopic marker for CH_3CO formation in the determination of photo-dissociation quantum yields for acetone,[10] an important source of HO*x* radicals and PAN ($CH_3C(O)O_2NO_2$) in the upper troposphere.[11,12] Recent studies on the yield of OH in the reaction between $CH_3C(O)O_2$ and HO_2 observed OH from (R1).[13] The title reaction will also have occurred in and potentially impacted on the results of studies of PAN formation in (R2) at low pressures where the yield of OH is large.

$$CH_3C(O)O_2 + NO_2 + M \leftrightarrow CH_3C(O)O_2NO_2 + M \quad (R2)$$

Max-Planck-Institut für Chemie, 55128 Mainz, Germany.
E-mail: john.crowley@mpic.de
† Present address: Department of Chemistry, University of York, York, YO10 5DD, UK.

For example, in their study of PAN formation, Bridier *et al.*[14] generated CH_3CO radical in the presence of O_2 to examine the kinetics of the reaction of $CH_3C(O)O_2 + NO_2$ (R2) at pressures down to 20 mbar. As the results of the present publication show, at such pressures 18% of CH_3CO reacting with O_2 forms OH instead of $CH_3C(O)O_2$. Data recorded at low pressure by Bridier *et al.* might thus be subject to systematic error since reaction channel (R1b) was not known to take place in 1991.

The reaction of $CH_3C(O)O_2$ with HO_2 (R3), which competes with (R2) at low NO*x* levels,[15] has drawn considerable interest in recent years.[13,16–18] Its main reaction channel (R3a) preserves a HO*x* species (HO*x* is OH + HO_2) and an organic radical and is hence radical-propagating, which helps sustain atmospheric oxidation capacity.

$$CH_3C(O)O_2 + HO_2 \rightarrow CH_3C(O)O + OH + O_2 \quad (R3a)$$

$$\rightarrow CH_3C(O)O_2H + O_2 \quad (R3b)$$

$$\rightarrow CH_3C(O)OH + O_3 \quad (R3c)$$

In experiments on (R3), $CH_3C(O)O_2$ and HO_2 are usually generated by reaction of Cl atoms with CH_3CHO and CH_3OH in air involving intermediate generation of CH_3CO and CH_2OH radicals. Therefore, OH-generation influences the initial $[CH_3C(O)O_2]/[HO_2]$-ratio in these experiments. In product studies that do not allow for an experimental separation between different OH-formation routes, (R1b) must be well known so that discrimination between OH formed in (R1b) and (R3a), respectively, is possible.

In the present work we employ a new experimental approach to quantify the pressure-dependence of the OH forming channels (R1b) and (R4b) of the reactions of O_2 with CH_3CO and its OH-substituted analogue $HOCH_2CO$.

$$HOCH_2CO + O_2 + M \rightarrow HOCH_2C(O)O_2 + M \quad (R4a)$$

$$\rightarrow OH + \cdots \quad (R4b)$$

We assume that, for reaction (R4), the same pathways are available as in (R1), *i.e.* competition between peroxy-radical formation and OH (see Scheme 1, R = $HOCH_2$). The formation of the peroxy radical, its UV-absorption spectrum and its reaction with HO_2 will be subject of a future publication from this group.

Throughout this work the branching ratios of the OH-forming reaction channels are defined as follows: $k_{1b}/k_1 = \alpha_{1b}$ and $k_{4b}/k_4 = \alpha_{4b}$.

2 Experimental

2.1 Experimental set-up

The experiments detailed in this publication were performed using the pulsed laser photolysis-laser induced fluorescence (PLP-LIF) apparatus that has been described previously[19,20] and only a short description is given here. Experiments were conducted in a 500 cm^3 reactor at room temperature. The pressure was monitored with a capacitance manometer, and gas flow rates were selected such that a fresh gas sample was available for photolysis at each laser pulse. Reactions were performed at pressures between 27 and 400 mbar in nitrogen and helium bath gases with added O_2 or in air.

Reactions were initiated by the 248 nm photolysis of H_2O_2 ($8–12 \times 10^{14}$ molecule cm^{-3}) or $COCl_2$ ($3–11 \times 10^{15}$ molecule cm^{-3}) using an excimer laser (Lambda Physik). Laser fluences of 39–55 mJ cm^{-2} per pulse resulted in formation of $0.3–0.5 \times 10^{12}$ OH radicals cm^{-3} or $1–5 \times 10^{12}$ Cl-atoms cm^{-3}. Two absorption cells located upstream of the reactor enabled on-line concentration measurements of the reactants at 185 nm and 214 nm. The optical path-lengths of the absorption cells are l_{185} = 43.8 cm and l_{214} = 34.8 cm.

Fluorescence from OH was detected by a photomultiplier tube shielded by a 309 nm interference filter and a BG 26 glass cut-off filter. The frequency doubled emission from a Nd-YAG-pumped dye laser (Quantel, Lambda Physik) was used to excite the $A^2\Sigma(\nu = 1) \leftarrow X^2\Pi(\nu = 0)$, Q_{11} (1) transition of OH at 281.997 nm.

2.2 Chemicals

Liquid samples of CH_3CHO (Roth, $\geq$99.5%) were degassed by repeated evacuation, and stored in a blackened glass bulb as $\sim$1% mixture in N_2. $HOCH_2CHO$ was prepared during the experiments from its dimer (Sigma-Aldrich) by heating the solid sample to 50–75 °C and eluting gaseous $HOCH_2CHO$ by a continuous flow of N_2. $COCl_2$ (Fluka, >99%) was stored in a stainless steel canister as $\sim$4% mixture in N_2 or He. H_2O_2 (AppliChem, 50%) was concentrated in vacuum to >80% and used as liquid sample. He (Westfalen, 99.999%), N_2 (Westfalen, 99.999%) and O_2 (Westfalen, 99.999%) were used as supplied.

3 Results

3.1 Experimental approach

We performed back-to-back experiments in reaction mixtures containing either H_2O_2 or $COCl_2$ as photolytic sources of OH radicals or Cl atoms. Addition of CH_3CHO or $HOCH_2CHO$ to the $COCl_2$ experiments converted Cl atoms into CH_3CO or $HOCH_2CO$, which reacted with O_2 to form OH. This allowed us to compare OH formation *via* title reactions (R1b) and (R4b) directly with OH production from H_2O_2-photolysis, a well-characterized source of OH radicals. Formation of acyl radicals by the reaction of Cl atoms with CH_3CHO ($\Delta H = -58$ kJ mol^{-1})[18] or $HOCH_2CHO$ ($\Delta H = -49$ kJ mol^{-1})[18,21] are exothermic processes and the nascent fragments are expected to be vibrationally and rotationally hot. Assuming an energy transfer efficiency of 300 cm^{-1} per collision with N_2, hot CH_3CO would be deactivated within 16 collisions, ensuring that, at the high pressures of bath gases used in this study, acetyl should, to a good approximation, be thermalized before reaction with O_2 takes place. Experiments in which N_2 was mixed with 1% O_2 yielded the same results as those with 21% O_2, so that no evidence was obtained for reaction of non-thermalised CH_3CO with O_2. Even in the experiments in He (presumably a less efficient energy transfer medium that N_2) no dependence of the OH-yield on O_2 partial pressure was obtained. We note also that the existence of a direct channel for OH-formation from excited CH_3CO and O_2 is considered unlikely.[9]

3.1.1 Determination of α. The OH-LIF system was calibrated by photolysing H_2O_2 that, at 248 nm, generates OH radicals with a quantum yield of 2.[22]

$$H_2O_2 + h\nu\ (248\ \text{nm}) \rightarrow 2OH \qquad \text{(R5)}$$

Quasi-instantaneous photolytic OH-formation and subsequent OH loss *via* (R6) result in a mono-exponential decay of [OH] that was recorded by OH-LIF.

$$OH + H_2O_2 \rightarrow HO_2 + H_2O \qquad \text{(R6)}$$

The LIF-signal is proportional to [OH] and was fitted by eqn (2) where f_{cal} is a calibration factor that quantifies the sensitivity of the LIF-system.

$$LIF(t) = f_{cal} \times [OH](t) = s_{OH} \times e^{-a_{OH} \cdot t} \qquad (2)$$

where a_{OH} and s_{OH} represent the fitted parameters. Due to the low conversion of H_2O_2 (<0.1%) its concentration, $[H_2O_2]$, can be considered constant over the course of the reaction. With $k_6' = k_6 \times [H_2O_2]$, and $[OH]_0$ as the initial OH concentration, the temporal evolution of [OH] can be described by the integrated rate law for first-order kinetics:

$$[OH](t) = [OH]_0 \times e^{-k_6' \cdot t} \qquad (3)$$

Combining eqn (2) and (3) we get:

$$f_{cal} \cdot [OH]_0 = s_{OH} \qquad (4)$$

In back-to-back experiments, H_2O_2 was replaced by $COCl_2$ and an acyl radical source (CH_3CHO or $HOCH_2CHO$). Photolysis of $COCl_2$ generates Cl atoms with a quantum yield of 2.[23,24]

$$COCl_2 + h\nu\ (248\ \text{nm}) \rightarrow 2Cl + CO \qquad \text{(R7)}$$

Reaction of Cl with CH_3CHO (R8) forms CH_3CO with a yield very close to unity ($k_8 = 8.0 \times 10^{-11}$ cm^3 molecule^{-1} s^{-1}).[17]

$$Cl + CH_3CHO \rightarrow CH_3CO + HCl \qquad \text{(R8)}$$

OH formation in reaction (R1b) and its main loss *via* reaction (R9) are both resolved on the time-scale of our experiments and a bi-exponential time-dependence of the LIF-signal is observed ($k_9 = 1.5 \times 10^{-11}$ cm^3 molecule^{-1} s^{-1}).[17,18]

$$OH + CH_3CHO \rightarrow CH_3CO + H_2O \qquad \text{(R9a)}$$

$$\rightarrow CH_2CHO + H_2O \qquad \text{(R9b)}$$

Reaction with OH generates mainly CH_3CO ($\alpha_{9a} = 0.95$) which is accounted for in the analytical expression of the [OH] time evolution presented below. Only 5% of the OH formed in (R1) is thus converted *via* (R9b) into CH_2CHO. Even if CH_2CHO were converted with unity yield into OH radicals, this would result in a maximum overestimation of no more than 5% in the value of α_{1b}.

Measured LIF-profiles were analysed using eqn (5).

$$LIF(t) = f_{cal} \times [OH](t) = s_{Cl}\frac{a_{Cl1}}{a_{Cl2} - a_{Cl1}}(e^{-a_{Cl1}t} - e^{-a_{Cl2}t}) \qquad (5)$$

where a_{Cl1}, a_{Cl2} and s_{Cl1} represent the fitted parameters. Under the assumptions that (R1) is fast compared to (R8) and (R9) and that $[CH_3CHO]$ remains constant on the experimental time-scale, an analytical expression for the temporal evolution of [OH] can be derived.

$$[OH](t) = \frac{\alpha_{1b} k_8' [Cl]_0}{(1 - \alpha_{1b}\alpha_{9a})k_9' - k_8'}\left(e^{-k_8' t} - e^{-(1-\alpha_{1b}\alpha_{9a})k_9' t}\right) \qquad (6)$$

In this expression, $k_8' = [CH_3CHO] \times k_8$, $k_9' = [CH_3CHO] \times k_9$ and $[Cl]_0$ is the Cl-concentration initially formed by photolysis. Conditions were chosen such that reaction (R1) was 5.2–250 times faster than (R8), and 28–1300 times faster than (R9) and thus fast on the experimental time-scale of ~1 ms. Combining eqn (5) and (6) we get:

$$\alpha_{1b} f_{cal} [Cl]_0 = s_{Cl} \qquad (7)$$

f_{cal} can be eliminated from eqn (7) by insertion of eqn (4) because experiments were conducted back-to-back.

$$\alpha_{1b} = \frac{s_{Cl}}{s_{OH}} \times \frac{[OH]_0}{[Cl]_0} \qquad (8)$$

This assumes that fluorescence quenching is dominated by the bath gas and that the contribution of reactants is negligible so that switching between H_2O_2 and $COCl_2$/aldehyde does not change the detection sensitivity to OH. The experiments performed in He, which is a weak quencher of OH-fluorescence, are the most likely to be influenced, should this not be the case. In Section 3.3 we show however that such quenching effects did not have a measurable effect on the results obtained.

The initial concentrations $[OH]_0$ and $[Cl]_0$ were calculated from $[H_2O_2]$ and $[COCl_2]$, the respective 248 nm cross sections and the number of photons per photolysis pulse n_{Phot}. We then derive:

$$\alpha_{1b} = \frac{s_{Cl}}{s_{OH}} \times \frac{\Phi^{248}_{H_2O_2} n_{Phot}\left(1 - e^{-\sigma^{248}_{H_2O_2}[H_2O_2]}\right)}{\Phi^{248}_{COCl_2} n_{Phot}\left(1 - e^{-\sigma^{248}_{COCl_2}[COCl_2]}\right)} = \frac{s_{Cl}}{s_{OH}} \times \frac{1 - e^{-\sigma^{248}_{H_2O_2}[H_2O_2]}}{1 - e^{-\sigma^{248}_{COCl_2}[COCl_2]}} \qquad (9)$$

Since the laser intensity remained stable (within ~1%) during back-to back experiments, n_{Phot} cancels out as do the quantum yields of OH formation $\left(\Phi^{248}_{H_2O_2}\right)$ and Cl formation $\left(\Phi^{248}_{COCl_2}\right)$ that both equal 2. The precursor concentrations $[H_2O_2]$ and $[COCl_2]$ were calculated from the respective optical depths $OD^{214}_{H_2O_2}$ and $OD^{214}_{COCl_2}$ measured at 214 nm in a separate absorption cell (see Section 2.1).

$$[precursor] = \frac{OD^{214}_{precursor}}{\sigma^{214}_{precursor} l_{214}} \qquad (10)$$

$HOCH_2CHO$ was used as acyl radical precursor in experiments for the determination of α_{4b}. Reaction of Cl atoms with $HOCH_2CHO$ (R10) forms $HOCH_2CO$ with a yield of

$\alpha_{10a} = 0.65$ ($k_{10} = 7.5 \times 10^{-11}$ cm^3 molecule^{-1} s^{-1}).[25,26] Reaction of HOCHCHO with O_2 (R11), is not known to form OH.[25,26]

$$Cl + HOCH_2CHO \rightarrow HOCH_2CO + HCl \quad (R10a)$$

$$\rightarrow HOCHCHO + HCl \quad (R10b)$$

$$HOCHCHO + O_2 \rightarrow HC(O)CHO + HO_2 \quad (R11)$$

Reaction with $HOCH_2CHO$ (R12) is the main OH loss channel in these experiments.

$$OH + HOCH_2CHO \rightarrow HOCH_2CO + H_2O \quad (R12a)$$

$$\rightarrow HOCHCHO + H_2O \quad (R12b)$$

Reaction with OH generates $HOCH_2CO$ with a higher yield ($\alpha_{12a} = 0.80$) than reaction with Cl. Based on this kinetic scheme, one again expects a bi-exponential time profile of [OH] that can be analysed by eqn (5). The temporal evolution of [OH] is described by the integrated rate law (11) which was derived analytically assuming reaction (R4) to be fast compared to reactions (R10) and (R12) and that [$HOCH_2CHO$] was not significantly depleted during the experiments.

$$[OH](t) = \frac{\alpha_{10a}\alpha_{4b}k_{10}'[Cl]_0}{(1-\alpha_{4b}\alpha_{12a})k_{12}' - k_{10}'}\left(e^{-k_{10}'t} - e^{-(1-\alpha_{4b}\alpha_{12a})k_{12}'t}\right) \quad (11)$$

with $k_{10}' = [HOCH_2CHO] \times k_{10}$ and $k_{10}' = [HOCH_2CHO] \times k_{12}$. Under the experimental conditions applied in this work and assuming the rate coefficients of (R1) and (R4) to be equal, (R4) was 12 to 280 times faster than (R10) and 110 to 2700 times faster than (R12) and, thus, fast on the experimental time-scale of $\sim$1 ms. As for the $CH_3CO + O_2$ system we can derive an analytical expression for α_{4b} from eqn (4) and (11).

$$\alpha_{4b} = \frac{1}{\alpha_{10a}} \cdot \frac{s_{Cl}}{s_{OH}} \cdot \frac{1 - e^{-\sigma^{248}_{H_2O_2}[H_2O_2]}}{1 - e^{-\sigma^{248}_{COCl_2}[COCl_2]}} \quad (12)$$

α_{4b} can thus be derived from measurement of $OD^{214}_{H_2O_2}$, $OD^{214}_{COCl_2}$, s_{OH} and s_{Cl}, the absorption cross sections of $COCl_2$ and H_2O_2 at 214 nm and 248 nm and the branching ratio α_{10a}.

3.1.2 Error estimation. The exponentials in eqn (9) and (12) can be expanded in a Taylor series that is stopped after the second term. By insertion of eqn (9) and (10) thus becomes

$$\alpha_{1b} \approx \frac{s_{Cl}}{s_{OH}} \cdot \frac{\sigma^{248}_{H_2O_2} \cdot \sigma^{214}_{COCl_2} \cdot OD^{214}_{H_2O_2}}{\sigma^{248}_{COCl_2} \cdot \sigma^{214}_{H_2O_2} \cdot OD^{214}_{COCl_2}} \quad (13)$$

Similarly, eqn (12) becomes

$$\alpha_{4b} \approx \frac{1}{\alpha_{10a}} \cdot \frac{s_{Cl}}{s_{OH}} \cdot \frac{\sigma^{248}_{H_2O_2} \cdot \sigma^{214}_{COCl_2} \cdot OD^{214}_{H_2O_2}}{\sigma^{248}_{COCl_2} \cdot \sigma^{214}_{H_2O_2} \cdot OD^{214}_{COCl_2}} \quad (14)$$

This allows us to separate statistical errors, *i.e.* reading errors or uncertainties in the determinations of s_{OH} and s_{Cl} which are small, from the systematic errors originating from uncertainties in literature values of the absorption cross sections and, in the case of α_{4b}, the branching ratio $\alpha_{10a} = 0.65 \pm 0.05$.[25] To reduce systematic error, absorption cross sections were taken from literature sources that specify values for both wavelengths used in this work. Values for H_2O_2 were taken from Vaghjiani *et al.*,[27] values for $COCl_2$ were taken from Meller *et al.* whose data are published in the MPI-Mainz UV/VIS Spectral Atlas[28] ($\sigma^{214}_{H_2O_2} = 33.0 \pm 2.2$, $\sigma^{248}_{H_2O_2} = 9.23 \pm 0.70$, $\sigma^{214}_{COCl_2} = 11.3 \pm 1.1$ and $\sigma^{248}_{COCl_2} = 8.96 \pm 0.90$ all values given in units of 10^{-20} cm^2 molecule^{-1}).

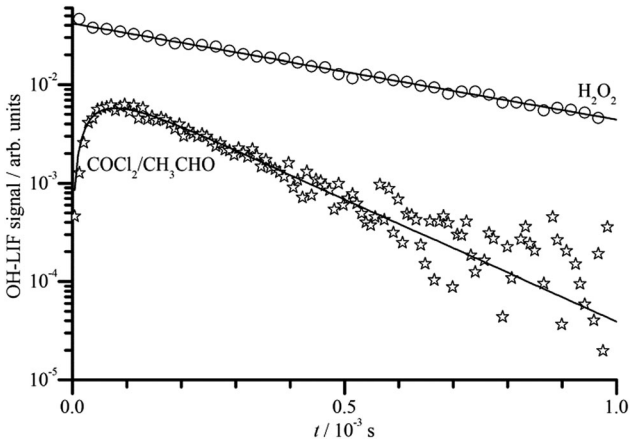

Fig. 1 OH-LIF profiles measured in back-to-back experiments in 133 mbar of N_2 bath gas with 1% O_2. The solid lines are fits to expressions (2) and (5).

3.2 $CH_3CO + O_2$ (N_2/O_2)

Back-to-back PLP-LIF-experiments on (R1) were performed at pressures between 133 and 270 mbar of N_2 or at 27 and 270 mbar of air. Fig. 1 shows a pair of OH-LIF time profiles recorded at 133 mbar in N_2. Both OH-profiles display the expected kinetics and were analysed using eqn (2) or (5), respectively. Although this work was not performed to re-measure the rate-coefficients of reactions (R8) and (R9), we did derive them from the fit-parameters and the respective [CH_3CHO] as a check of our experimental approach. We obtained $k_8 = (7.4 \pm 1.1) \times 10^{-11}$ cm^3 molecule^{-1} s^{-1}, and $k_9 = (1.8 \pm 0.2) \times 10^{-11}$ cm^3 molecule^{-1} s^{-1} where the uncertainties represent statistical errors (2σ) in the fit-parameters only. [CH_3CHO] was determined barometrically and carries an additional uncertainty of $\sim$20%. Our values are, within these uncertainties, in accordance with the currently recommended literature values of $k_{8,Lit} = (8.0^{+1.4}_{-1.2}) \times 10^{-11}$ cm^3 molecule^{-1} s^{-1}, and $k_{9,Lit} = (1.5 \pm 0.2) \times 10^{-11}$ cm^3 molecule^{-1} s^{-1}.[17,18]

Fig. 2 shows the results of all single experiments as a plot of the reciprocal of α_{1b} against [M]. A linear regression of the data resulted in (all errors statistical, 2σ)

$$\alpha_{1b}^{-1}(N_2) = (0.55 \pm 1.81) + (9.52 \pm 0.72) \times 10^{-18}\ cm^3\ molecule^{-1}\ [M]$$

As expected[3,5,29] the intercept is 1 within statistical uncertainty. We then re-fitted the data using eqn (1), *i.e.* we performed another linear regression with the intercept being fixed to 1 (thick solid line in Fig. 2). From this we obtain $\frac{k_M}{k_D} = (9.4 \pm 0.48) \times 10^{-18}$ cm^3 molecule^{-1} (error statistical only, 2σ). We applied eqn (13) to incorporate the systematic uncertainties (2σ) and derive a final value of $\frac{k_M}{k_D} = (9.4 \pm 1.7) \times 10^{-18}$ cm^3 molecule^{-1}. In Fig. 2 these error margins are represented by thin solid lines.

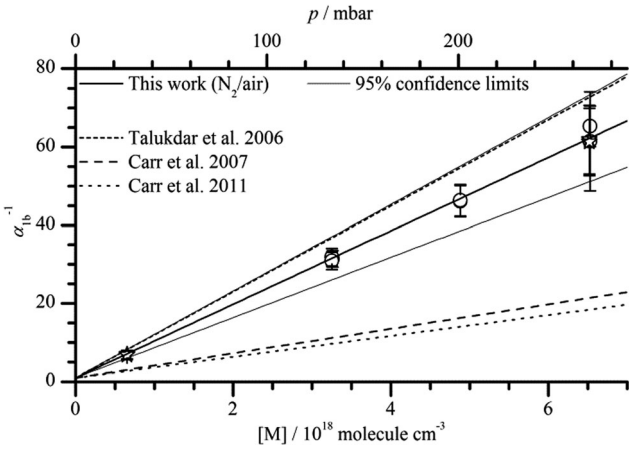

Fig. 2 Plot of α_{1b}^{-1} *versus* bath gas number density [M] at 296 K. Talukdar *et al.* (2006).[34] Carr *et al.* (2007).[3] Carr *et al.*, (2011).[2] The stars represent data obtained in air, the circles represent data obtained in a mixture of oxygen (1%) in N_2.

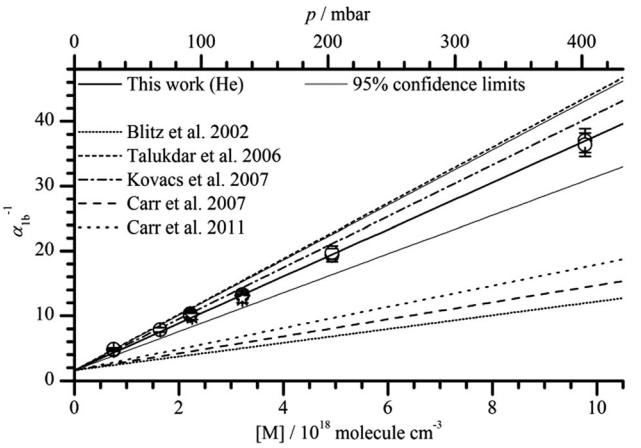

Fig. 3 Plot of α_{1b}^{-1} against bath gas number density [M] or pressure. Data were recorded in He with addition of 1.3 mbar (stars) or 2.7 mbar (circles) of O_2. Note that the literature data are plotted with an intercept of 1.6 to take into account the effect of quenching by O_2 (see text for details). Blitz *et al.* (2002).[4] Talukdar *et al.* (2006).[34] Kovács *et al.* (2007).[6] Carr *et al.* (2007).[3] Carr *et al.* (2011).[2]

We note that the data show no dependence on the O_2 concentration and that values of α_{1b} determined in air would be higher if CH_3CO were not thermalized and if there were an additional OH-formation route *via* $CH_3CO^{\#} + O_2$. This observation rules out a significant contribution of hot acetyl radicals.

3.3 $CH_3CO + O_2$ (He)

Back-to-back PLP-LIF-experiments on (R1) were performed at pressures between 33 and 400 mbar of He. From the fit-parameters and the respective [CH_3CHO] we derived $k_8 = (7.6 \pm 0.4) \times 10^{-11}$ cm^3 molecule^{-1} s^{-1}, and $k_9 = (1.9 \pm 0.1) \times 10^{-11}$ cm^3 molecule^{-1} s^{-1} where the uncertainties represent statistical errors (2σ) in the fit-parameters, only. As described above, [CH_3CHO] was determined from barometric and mass flow readings and carries an additional uncertainty of $\sim$20%. These values are, within combined uncertainties, in accordance with the currently recommended literature values.

Fig. 3 shows the results of all experiments performed in He with an addition of 2.7 (or 1.3) mbar of O_2 as a plot of the reciprocal of α_{1b} against He number density [M]. For the experiments with 2.7 mbar O_2, a linear regression of the data resulted in (all errors statistical, 2σ)

$$\alpha_{1b}^{-1}(\mathrm{He}) = (2.13 \pm 0.35) + (3.52 \pm 0.19) \times 10^{-18}\ \mathrm{cm^3\ molecule^{-1}}\ [\mathrm{M}]$$

The two data points obtained using 1.3 mbar of O_2 reveal the expected trend, slightly enhanced yields (but a similar slope) due to the quenching effect of O_2. With 2.7 mbar of O_2 we expect α_{1b}^{-1} to approach 1.6 ± 0.11 (the value we derive from $\frac{k_M}{k_D}$-value for N_2 and air) at zero pressure. Within the statistical uncertainties the intercept (2.13 ± 0.35) is however slightly higher than this. In the experiments in He, the main contribution to OH-fluorescence quenching is O_2 and not the H_2O_2 and CH_3CHO and Cl_2CO reactants. The fact that the two datasets obtained with different O_2 concentrations are in good agreement, supports this.

We therefore re-fitted the data using eqn (1), *i.e.* we performed another linear regression with the intercept being fixed to 1.6 (thick solid line in Fig. 3). From this we derived $\frac{k_M}{k_D} = (3.62 \pm 0.05) \times 10^{-18}$ cm^3 molecule^{-1} (error statistical only, 2σ). We applied eqn (13) to incorporate the systematic uncertainties (2σ) and derived a final value of $\frac{k_M}{k_D} = (3.6 \pm 0.6) \times 10^{-18}$ cm^3 molecule^{-1}. In Fig. 3 these error margins are represented by thin solid lines.

3.4 $HOCH_2CO + O_2$ (N_2/O_2)

Back-to-back PLP-LIF-experiments using $HOCH_2CHO$ as acyl radical precursor were performed at pressures between 33 and 269 mbar in N_2 or air. Fig. 4 shows a pair of OH-LIF time profiles recorded at 133 mbar in N_2 which were fitted using eqn (2) or (5), respectively. As a check for possible error sources

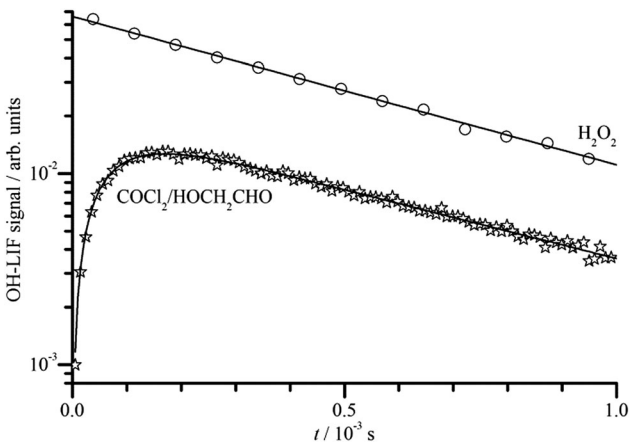

Fig. 4 OH-LIF profiles measured in back-to-back experiments at 133 mbar of N_2 bath gas containing 2.7 mbar of O_2. The solid lines are fits using equations (2) and (5).

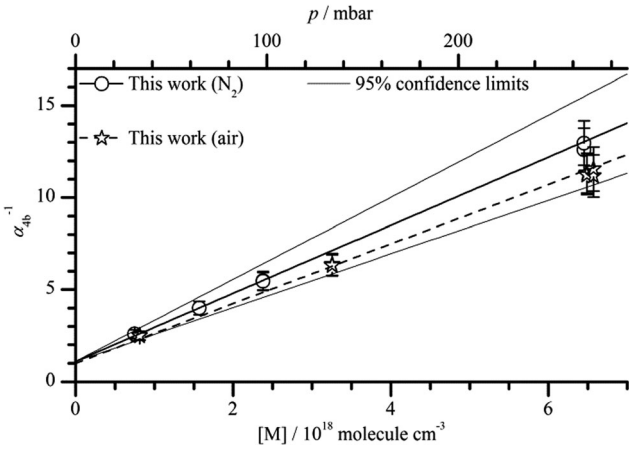

Fig. 5 Plot of α_{4b}^{-1} *versus* bath gas number density [M] or pressure, respectively.

of our experimental approach, we derived the rate-coefficients of reactions (R10) and (R12) from the fit-parameters and the respective [$HOCH_2CHO$], we get $k_{10} = (6.6 \pm 0.3) \times 10^{-11}$ cm^3 molecule^{-1} s^{-1}, and $k_{12} = (1.0 \pm 0.2) \times 10^{-11}$ cm^3 molecule^{-1} s^{-1} where the uncertainties represent statistical errors (2σ) in the fit-parameters, only. [$HOCH_2CHO$] was derived by measuring its absorption at 185 nm using a literature value for the absorption cross section of $HOCH_2CHO$ ($\sigma^{185}_{HOCH_2CHO} = (3.85 \pm 0.20) \times 10^{-18}$ cm^2 molecule^{-1})[30] and carries an additional uncertainty of ~10%. Our values are, within combined uncertainties, in accordance with the currently recommended literature values of $k_{10,Lit} = (7.6 \pm 1.5) \times 10^{-11}$ cm^3 molecule^{-1} s^{-1},[26] and $k_{12,Lit} = (0.80^{+0.33}_{-0.23}) \times 10^{-11}$ cm^3 molecule^{-1} s^{-1}.[17,18]

Fig. 5 shows the results of all single determinations of α_{4b} plotted as α_{4b}^{-1} against [M]. Except for the data measured at the lowest pressure of 33 mbar, the values for α_{4b} determined in air are slightly higher than those measured in nitrogen. We therefore evaluated data recorded in N_2 or air separately to check if the final results differ within their statistical uncertainties. A linear regression of the data obtained in N_2 gave (all errors statistical, 2σ)

$$\alpha_{4b}^{-1}(N_2) = (1.23 \pm 0.42) + (1.78 \pm 0.26) \times 10^{-18}\ \text{cm}^3\ \text{molecule}^{-1}\ [\text{M}]$$

A linear regression of the data obtained in air resulted in (all errors statistical, 2σ)

$$\alpha_{4b}^{-1}(\text{air}) = (1.24 \pm 0.43) + (1.55 \pm 0.19) \times 10^{-18}\ \text{cm}^3\ \text{molecule}^{-1}\ [\text{M}]$$

Assuming that (R4b) forms OH with unity yield at pressures approaching 0 mbar, we expect the intercept to be unity in air which, within statistical uncertainty, is the case. In the N_2-experiments a constant amount of 2.7 mbar of O_2 was added. Thus, at [M] = 0 molecule cm^{-3} we expect α_{4b}^{-1} to approach ~1.1, *i.e.* the value we derived using [M] = 6.5×10^{16} molecule cm^{-3} and $\frac{k_M}{k_D} = 1.6 \times 10^{-18}$ cm^3 molecule^{-1}. This is also confirmed by the data. In both cases we performed linear regressions according to eqn (1), with the intercept being fixed to 1.1 for the data recorded in N_2, and to unity for the air-data. We derived

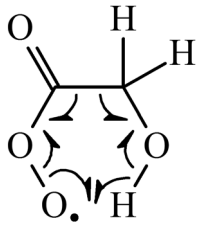

Scheme 2 Possible transition state for OH formation in (R4b).

$\frac{k_M}{k_D} = (1.85 \pm 0.16) \times 10^{-18}$ cm^3 molecule^{-1} (solid black line in Fig. 5) for the data recorded in nitrogen and $\frac{k_M}{k_D} = (1.62 \pm 0.14) \times 10^{-18}$ cm^3 molecule^{-1} (dashed black line) for the data recorded in air (errors are statistical, 2σ). Within combined uncertainties measurements in nitrogen and air resulted in the same values of $\frac{k_M}{k_D}$ and, accordingly, α_{4b}.

The slightly larger α_{4b}-values observed at higher pressures in air are potentially due to experimental scatter. Our data do not however allow us to completely rule out the existence of an additional, O_2-dependent OH-source as the cause. Therefore, we decided to rely exclusively on the data recorded in N_2 (with 1–10% of O_2 added) which would be less impacted by such an additional OH-source. Doing so we commit a maximum error of 7% in α_{4b} compared to values derived from all data. The fact that the data obtained at a fixed O_2-to-N_2 ratio of 21%, but at various pressures (and thus at different O_2 concentrations), display no significant deviation from the expected behaviour, suggests that an additional OH forming channel that is dependent on the O_2 partial pressure is not significant. Incorporation of systematic uncertainties (2σ), results in a final value of $\frac{k_M}{k_D} = (1.85 \pm 0.38) \times 10^{-18}$ cm^3 molecule^{-1}. The error margins that also enclose the data recorded in air are presented in Fig. 5 by thin solid lines.

Our studies on OH formation in the reactions of CH_3CO (R1) and $HOCH_2CO$ (R4) with O_2 reveal a strong dependence of the yield on substituents, with $\frac{k_M}{k_D}$ for (R4) a factor of 5 smaller than for (R1). Under the assumption that the collisional quenching of both activated peroxy radicals proceeds at a similar rate this large difference can be attributed to a more efficient decomposition of $HOCH_2C(O)O_2^{\#}$ compared to $CH_3C(O)O_2^{\#}$. This may be rationalized in terms of a more favourable reaction pathway in which the hydroxyl group of $HOCH_2C(O)O_2$ enables formation of a six-membered transition state as illustrated in Scheme 2 in which highly stable products (formaldehyde and CO_2) are formed along with OH.

4 Comparison with literature

4.1 $CH_3CO + O_2$

Several experimental studies have reported OH formation *via* (R1b) in N_2, O_2 and He.[2–6] Table 1 and Fig. 2 and 3 summarise

Table 1 Summary of results (all room temperature) and comparison with literature

	M	This work	Tyndall (1997)	Blitz (2002)	Talukdar (2006)	Kovács (2007)	Carr (2007)	Carr (2011)	Groß (2014)
CH_3CO									
k_M/k_D [a]	N_2	9.4 ± 1.7	(5.9)[b]		11.0 ± 2.5		3.59 ± 0.60	2.67 ± 1.40	(~9)[d]
	He	3.6 ± 0.6		1.06 ± 0.05	4.3 ± 1.0	3.9 ± 0.6[c]	1.31 ± 0.51	1.63 ± 0.54	
Ratio N_2/He		2.6			2.6		2.7	1.6	
$HOCH_2CO$									
k_M/k_D [a]	N_2	1.85 ± 0.38							

Tyndall (1997),[5] Blitz (2002),[4] Talukdar (2006),[34] Kovács (2007),[6] Carr (2007),[3] Carr (2011),[2] Groß (2014).[13] [a] Units of 10^{-18} cm^3 $molecule^{-1}$. [b] The cited value is based on a correction from G. S. Tyndall that was published by Carr *et al.*[3] [c] Value obtained by applying eqn (1) to the data of Kovács *et al.*[6] [d] Value derived from a single experiment at 233 mbar in N_2/O_2.

the $\frac{k_M}{k_D}$-values from these studies as well as those from our work. Note that in Fig. 3 the literature data are plotted with an intercept of 1.6 to take into account the presence of O_2 in our experiments at extrapolated zero mbar of He.

Tyndall *et al.*[5] studied the reaction of Cl atoms with CH_3CHO by irradiation of Cl_2–CH_3CHO-mixtures in N_2 or O_2 in environmental chambers and analysed the reaction mixtures by infra-red absorption spectroscopy. They found a pressure-dependence of the apparent rate coefficient of (R8) when the experiments were performed in O_2 but none for the measurements in N_2. The value measured in O_2 increased if the experimental pressure was decreased; at 1.6 mbar the apparent rate coefficient was 2.7 times higher than that derived in N_2. The authors attributed these findings to OH formation in (R1b). Thus, they did not directly detect OH, but their kinetic and product studies provided strong evidence for OH formation. The $\frac{k_M}{k_D}$-value shown in Table 1 was derived by Carr *et al.*[3] based on a personal communication with Tyndall *et al.*[5]

Blitz *et al.*[4] used the 248 nm pulsed laser photolysis of $CH_3C(O)CH_3$ in He to generate CH_3CO and used OH-LIF for the detection of hydroxyl radicals formed in (R1b) at pressures between 13–533 mbar. Calibration of the LIF-system was achieved by fixing α_{1b} at zero pressure to unity, which neglects to take into account the fact that the acetyl radical yield is pressure dependent as a significant (but variable) fraction thermally decomposes to CH_3 and CO, at least in nitrogen bath gas.[31–33] Blitz *et al.* could thus have underestimated the value of KM/KD by about 16%.[3]

Talukdar *et al.*[34] used different photolytic schemes (photolysis of acetone, Cl + CH_3CHO and OH + CH_3CHO) for CH_3CO generation coupled to OH-LIF to investigate OH-formation or modification of OH kinetics due to (R1) at experimental pressures between 27–800 mbar in He, N_2 and O_2. The resulting $\frac{k_M}{k_D}$ values are in good agreement with our results.

Kovács *et al.*[6] used two low-pressure fast discharge flow tubes (operated at pressures between 1.3 and 11 mbar in helium) that were equipped with LIF or resonance fluorescence detection of OH radicals. CH_3CO was formed by reacting CH_3CHO with OH that was generated from H and NO_2, or from F and H_2O. The authors compared decay rates of OH radicals with or without O_2 present in the reaction mixture. We applied eqn (1) to the α_{1b}-data provided by Kovács *et al.* to derive a value of $\frac{k_M}{k_D}$ that is in good agreement with those presented by Talukdar *et al.* and this work.

Carr *et al.*[3] used the 248 nm pulsed laser photolysis of $CH_3C(O)OH$ to generate prompt OH and CH_3CO radicals in equal amounts. Detection of OH radicals was achieved by OH-LIF. Experiments were restricted to pressures of <138 mbar of He, or <34 mbar of N_2. The approach is self-calibrated since it allows comparison of prompt OH formed in the photolysis step to OH formed from acetyl + O_2 and thus requires only separation of the LIF signal into prompt and slow components. Errors in the separation of prompt and slower OH contributions would thus affect α_{1b} two-fold and would be manifest at higher pressures of N_2 where the yield of OH is small. The resulting value for $\frac{k_M}{k_D}$ agrees well with the previous one of Blitz *et al.* from the same lab but accordingly differs by a factor of ~3 from our values.

Carr *et al.*[2] photolysed acetone at 248 nm to form CH_3CO and used OH-LIF detection. The resulting OH time profiles were fitted by a bi-exponential equation similar to the one presented here. Relative values of α_{1b} were measured in the pressure range of 7–400 mbar and based on an absolute scale by setting α_{1b} at 0 mbar to unity. Data were corrected by 25–35% for a pressure-dependence[23,31] in the CH_3CO yield of acetone photolysis. In their N_2-experiments the authors needed to make an additional correction since they observed a decrease of LIF-sensitivity at elevated pressures. The correction factors were derived in separate experiments by measuring OH-formation from 248 nm photolysis of *t*-butylhydroperoxide at the same pressure.

Although not a detailed study of the OH yield in the title reaction, we recently published data on OH formation in the reaction of HO_2 with $CH_3C(O)O_2$ (ref. 13) and also observed (in this case "unwanted") OH-formation *via* (R1b). This work was conducted in a different apparatus and used a different CH_3CO-formation scheme (355 nm-pulsed photolysis of CH_3CHO–CH_3OH–Cl_2–O_2–N_2-mixtures). OH was detected by an OH-LIF-unit that was calibrated by measuring OH from the reaction of HO_2 with NO. In spite of the different experimental approach we could accurately simulate the OH signals due to reaction (R1b) with the OH yield presented in the current work (see Fig. 8 in Groß *et al.*[13]). Use of α from the more recent publication of Carr *et al.*[2] would have resulted in an overestimation of initial OH-formation by a factor of 3.

Our results are in good agreement with those of Talukdar *et al.*[34] and Kovács.[6] We cannot explain the differences between our work and that of Blitz *et al.*[4] and Carr *et al.*[2,3] but we highlight the fact that no correction needs to be applied to our data.

In Table 1 we also show the ratio of the respective $\frac{k_M}{k_D}$ values in N_2 and He bath gases. From our data we derive a value of 2.6 which is in agreement with those of Talukdar *et al.* (2.7) and the 2007 study of Carr *et al.* 2007 (2.6). From the 2011 dataset of Carr *et al.* we derive a lower value of 1.6.

4.2 $HOCH_2CO + O_2$

Butkovskaya *et al.*[35] investigated the OH-initiated oxidation of $HOCH_2CHO$ in a turbulent flow reactor at 267 mbar of N_2. A chemical ionisation mass spectrometer was used to detect OH and derive a yield of α_{4b} = 22%. This high yield may reflect the fact that Butkovskaya *et al.*[35] were unaware that the reaction of $HOCH_2C(O)O_2$ with HO_2 (formed at a yield of 20% from OH + $HOCH_2CHO$ in the presence of O_2) forms OH with a yield of $\sim$70%.[16,36]

OH formation has also been observed[37] in the reaction of O_2 with CH_3OCO, which is isomeric with $HOCH_2CO$. Similar to (R4), OH-formation is accompanied by CH_2O and CO_2 by-products. The value of $\frac{k_M}{k_D}$ reported, $(7.4 \pm 1.9) \times 10^{-18}$ cm^3 molecule^{-1}, is four times larger than our value for $HOCH_2CO$. Given that the products of decomposition are identical the difference must be related to energetic differences in the transition state leading to dissociation.

5 Conclusion

We determined the pressure-dependence of the OH-forming branching ratios α_{1b} of reaction (R1a) and α_{4b} reaction (R4b) using a novel experimental approach. The values for α_{1b} are in accordance with some earlier studies[6,34] but clearly differ from those from the Leeds group[2–4] that derive much higher OH yields. Our data for α_{4b} show that hydroxylation of CH_3CO enhances OH-formation in the reaction with O_2 by approximately a factor of five.

Acknowledgements

We thank Jim Burkholder (National Oceanic and Atmospheric Administration, Boulder, CO) for sending us a copy of a poster "Determination of the OH Radical Yield in the $CH_3CO + O_2 + M$ Reaction" presented at the 19th International Symposium on Gas Kinetics in 2006. C. B. M. G. thanks the International Max Planck Research School for Atmospheric Chemistry and Physics for financial support.

References

1 G. S. Tyndall, T. A. Staffelbach, J. J. Orlando and J. G. Calvert, *Int. J. Chem. Kinet.*, 1995, **27**, 1009–1020.
2 S. A. Carr, D. R. Glowacki, C.-H. Liang, M. T. Baeza-Romero, M. A. Blitz, M. J. Pilling and P. W. Seakins, *J. Phys. Chem. A*, 2011, **115**, 1069–1085.
3 S. A. Carr, M. T. Baeza-Romero, M. A. Blitz, M. J. Pilling, D. E. Heard and P. W. Seakins, *Chem. Phys. Lett.*, 2007, **445**, 108–112.
4 M. A. Blitz, D. E. Heard and M. J. Pilling, *Chem. Phys. Lett.*, 2002, **365**, 374–379.
5 G. S. Tyndall, J. J. Orlando, T. J. Wallington and M. D. Hurley, *Int. J. Chem. Kinet.*, 1997, **29**, 655–663.
6 G. Kovács, J. Zádor, E. Farkas, R. Nádasdi, I. Szilágyi, S. Dóbé, T. Bérces, F. Márta and G. Lendvay, *Phys. Chem. Chem. Phys.*, 2007, **9**, 4142–4154.
7 J. Lee, C.-J. Chen and J. W. Bozzelli, *J. Phys. Chem. A*, 2002, **106**, 7155–7170.
8 H. Hou, A. Li, H. Hu, Y. Li, H. Li and B. Wang, *J. Chem. Phys.*, 2005, **122**, 224304.
9 A. Maranzana, J. R. Barker and G. Tonachini, *Phys. Chem. Chem. Phys.*, 2007, **9**, 4129–4141.
10 M. A. Blitz, D. E. Heard, M. J. Pilling, S. R. Arnold and M. P. Chipperfield, *Geophys. Res. Lett.*, 2004, **31**, L06111.
11 H. B. Singh, M. Kanakidou, P. J. Crutzen and D. J. Jacob, *Nature*, 1995, **378**, 50–54.
12 S. A. McKeen, T. Gierzak, J. B. Burkholder, P. O. Wennberg, T. F. Hanisco, E. R. Keim, R.-S. Gao, S. C. Liu, A. R. Ravishankara and D. W. Fahey, *Geophys. Res. Lett.*, 1997, **24**, 3177–3180.
13 C. B. M. Groß, T. J. Dillon, G. Schuster, J. Lelieveld and J. N. Crowley, *J. Phys. Chem. A*, 2014, **118**, 974–985.
14 I. Bridier, F. Caralp, H. Loirat, R. Lesclaux, B. Veyret, K. H. Becker, A. Reimer and F. Zabel, *J. Phys. Chem.*, 1991, **95**, 3594–3600.
15 G. J. Phillips, N. Pouvesle, J. Thieser, G. Schuster, R. Axinte, H. Fischer, J. Williams, J. Lelieveld and J. N. Crowley, *Atmos. Chem. Phys.*, 2013, **13**, 1129–1139.
16 D. Taraborrelli, M. G. Lawrence, J. N. Crowley, T. J. Dillon, S. Gromov, C. B. M. Groß, L. Vereecken and J. Lelieveld, *Nat. Geosci.*, 2012, **5**, 190–193.
17 R. Atkinson, D. L. Baulch, R. A. Cox, J. N. Crowley, R. F. Hampson, R. G. Hynes, M. E. Jenkin, M. J. Rossi and J. Troe, *Atmos. Chem. Phys.*, 2006, 3625–4055.
18 M. Ammann, R. A. Cox, J. N. Crowley, M. E. Jenkin, A. Mellouki, M. J. Rossi, J. Troe and T. J. Wallington, IUPAC Task Group on Atmospheric Chemical Kinetic Data Evaluation, 2014, http://iupac.pole-ether.fr/index.html.
19 T. J. Dillon, M. E. Tucceri and J. N. Crowley, *Phys. Chem. Chem. Phys.*, 2006, **8**, 5185–5198.
20 T. J. Dillon, A. Horowitz and J. N. Crowley, *Chem. Phys. Lett.*, 2007, **443**, 12–16.
21 A. Galano, J. R. Alvarez-Idaboy, M. E. Ruiz-Santoyo and A. Vivier-Bunge, *J. Phys. Chem. A*, 2005, **109**, 169–180.
22 R. Atkinson, D. L. Baulch, R. A. Cox, J. N. Crowley, R. F. Hampson, R. G. Hynes, M. E. Jenkin, M. J. Rossi and J. Troe, *Atmos. Chem. Phys.*, 2004, **4**, 1461–1738.
23 V. Khamaganov, R. Karunanandan, A. Horowitz, T. J. Dillon and J. N. Crowley, *Phys. Chem. Chem. Phys.*, 2009, **11**, 6173–6181.
24 C. Maul and K.-H. Gericke, *Int. Rev. Phys. Chem.*, 1997, **16**, 1–79.

25 H. Niki, P. D. Maker, C. M. Savage and M. D. Hurley, *J. Phys. Chem.*, 1987, **91**, 2174–2178.
26 C. Bacher, G. S. Tyndall and J. J. Orlando, *J. Atmos. Chem.*, 2001, **39**, 171–189.
27 G. L. Vaghjiani and A. R. Ravishankara, *J. Geophys. Res.: Atmos.*, 1989, **94**, 3487–3492.
28 H. Keller-Rudek, G. K. Moortgat, R. Sander and R. Sörensen, *Earth Syst. Sci. Data*, 2013, **5**, 365–373.
29 J. V. Michael, D. G. Keil and R. B. Klemm, *J. Chem. Phys.*, 1985, **83**, 1630–1636.
30 R. Karunanandan, D. Hölscher, T. J. Dillon, A. Horowitz, J. N. Crowley, L. Vereecken and J. Peeters, *J. Phys. Chem. A*, 2007, **111**, 897–908.
31 V. Khamaganov, R. Karunanandan, A. Rodriguez and J. N. Crowley, *Phys. Chem. Chem. Phys.*, 2007, **9**, 4098–4113.
32 H. Somnitz, T. Ufer and R. Zellner, *Phys. Chem. Chem. Phys.*, 2009, **11**, 8522–8531.
33 B. Rajakumar, T. Gierczak, J. E. Flad, A. R. Ravishankara and J. B. Burkholder, *J. Photochem. Photobiol., A*, 2008, **199**, 336–344.
34 R. K. Talukdar, M. E. Davis, L. Zhu, A. R. Ravishankara and J. B. Burkholder, *19th International Symposium on Gas Kinetics*, Orleans, France, 2006.
35 N. I. Butkovskaya, N. Pouvesle, A. Kukui and G. Le Bras, *J. Phys. Chem. A*, 2006, **110**, 13492–13499.
36 C. B. M. Groß, Fachbereich Chemie der Johannes-Gutenberg-Universität Mainz, Kinetische Studien zur OH-Bildung über die Reaktionen von HO_2 mit organischen Peroxyradikalen, PhD thesis, 2013.
37 J. C. Hansen, Y. Li, C. M. Rosado-Reyes, J. S. Francisco, J. J. Szente and M. M. Maricq, *J. Phys. Chem. A*, 2003, **107**, 5306–5316.